An Analysis of the Chemical-Mechanical Polishing Process *

Len Borucki† Cameron Connell ‡ Hala Jadallah §
Jianbo Li ¶ Peter J. Park ‖ Boris Petracovici **
David Zeigler ††

August 5, 1998

Abstract

We examine the non-uniform wear of the wafer and the pad in the Chemical Mechanical Polishing of wafers in the semiconductor industry. We model the pad as a set of springs in order to get the pressure distribution, which then determines the wear according to Preston's Law. The shape of the pad and the wafer evolve in time, as the wafer rotates and oscillates, and the pad rotates. The non-planarity that our model predicts resembles experimental data.

1 Introduction

In the semiconductor industry, it is necessary to generate surfaces with minimum topography. As the size of the structures on the circuit devices decreases, it is becoming even more important that the surfaces be made uniformly planar. Many techniques have been developed for this purpose, but most are ineffective in global planarization. The current standard method for planarization is the Chemical-Mechanical Polishing (CMP), which have been shown to yield the best results for wafer planarity and uniformity [1, 2, 3].

In the CMP process, a wafer is pressed against a pad while each is rotating about its axis. In practice, they rotate at the same angular speed since this gives

*This work was done while the authors were participating in the Mathematical Modeling in Industry Workshop for Graduate Students at the Institute for Mathematics and its Applications at the University of Minnesota

†Motorola (ryks90@email.sps.mot.com)
‡New York University (connellc@cims.nyu.edu)
§Indiana University (hjadalla@indiana.edu)
¶University of Kentucky (ljb@ms.uky.edu)
‖California Institute of Technology (pjpark@ama.caltech.edu)
**University of Illinois at Urbana (petracov@math.uiuc.edu)
††Texas A&M University (zeigler@math.tamu.edu)

constant relative speed for all points on the wafer. The wafer also moves back and forth along the line that connects the two centers. The pad is covered with slurry, which induces chemical reactions on the surface and plays an important role in the local planarization. The dimensions of the wafer, the pad, and the movements are shown in Fig. 1. Typically, each wafer requires about 60 rotations. Each pad can be used to polish about 150 wafers. After the non-uniformity of the surface exceeds given tolerance, the pad is discarded.

There are two main approaches to studying the CMP and in particular the determination of the pressure distribution [4]. One is to concentrate on the motion of slurry and the hydrodynamic and chemical interactions. For example, elastic contact surface mechanics and hydrodynamic lubrication were used to study the effect of suction fluid pressure below the wafer in [5]. Many authors have documented experiments in which the effect of the size and the concentration of the slurry particles on the wear were examined.

The other is the direct wafer-pad contact and the mechanical properties. A statistical model for the asperities was studied to characterize the surface roughness and its effect on the polishing rate [6]; Von Mises stress on the wafer surface is considered in [7]; mechanical properties of the slurry particles was studied in [8]; contact pressure and wafer shape changes were computed in [9].

While this method has been studied widely, a time-dependent simulation accounting for the rotations and the oscillation has not been performed until now.

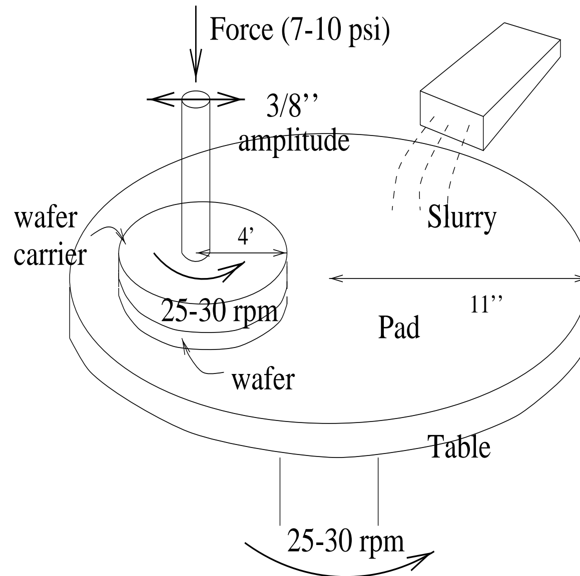

Figure 1: Schematic of the CMP Process

2 Formulation of the Problem

We would like to construct a model that describes the following two phenomena:

1. the shape and polishing rate of the wafer as a function of radial distance from the pad center.

2. the shape of the pad and wear-out rate, also as a function of radial distance from the pad center.

In the process of modeling one has to take into account the following factors:

- as the pad is used, the asperities wear down and the removal rate of the pad decreases;

- a worn pad is no longer planar. One expects a parabolic-type shape after a number of wafers have been polished. Therefore, the polishing rate at the edge of the wafer might exceed the rate at the center;

- as the pad rotates, points situated at different radii from the center will have different contact time with the wafer. This fact also influences the wear of the pad.

There are many different interactions in the pad-wafer problem. For example, at the microscopic scale, there are asperities, slurry, chemical reactions with the wafer, and the accumulation of debris in the pad pores which will all affect the removal rate. On the other hand, at the macroscopic level, contact time, distribution of pressure, relative velocity, and the radial oscillation of the wafer with respect to the pad must all be taken into account.

The literature we have consulted is extensive. However, most of the papers were limited in scope and handled the problem in a static sense. So a logical progression led us to attempt a dynamic approach.

The main steps to be followed are:

(i) start with a perfectly flat pad and a flat (at the macroscopic level) wafer. Consider a radial slice of the pad and wafer along a common diameter (Fig. 6);

(ii) apply an initial force, F, uniformly distributed on the wafer, which will determine a penetration, c, into the pad;

(iii) using the elasticity equations, with boundary conditions, find the displacements of the pad;

(iv) find the stress tensor, and the pressure distribution, as a function of distance from the center of the pad;

(v) using Preston's Law, find the removal rate and the change in profile of both the pad and the wafer;

(vi) update the profile of the pad and wafer and, assuming the applied force is constant, calculate the penetration.

By repeating steps (iii) through (vi), we can define a dynamic model which would reflect several intermediate profiles.

Since there does not exist an explicit solution for the general elasticity equation for the given boundary condition, we must approximate these values. Two different approaches were developed:

- the one-dimensional elasticity problem (spring equation) has an explicit solution. So one idea was to consider a "mattress" approximation of the pad: define a mesh on the pad and regard each element as a spring on the pad;
- Solve the plane-strain formulation of the elasticity problem using the boundary element method.

Each one of these approaches will be discussed later.

2.1 Relative Velocities

The removal rate depends on the relative velocities between the pad and the wafer. It is easy to show that the relative velocity is simply the same unidirectional vector for all points on the wafer. In Fig. 2, the velocity of the point P relative to the center of the pad is $V_p = \omega(-y-d, x)$ and relative to the center of the wafer $V_w = \omega(-y, x)$, where d is the distance between the two centers and ω is the angular velocity. By subtracting the two, we immediately see that the net velocity is always to the left. With the oscillation of the wafer at a constant speed, relative velocity is still the same for all points on the wafer.

2.2 Contact Time

2.2.1 Without oscillatory motion

The wafer rotates with ω_1 and oscillates up and down with ω_h, while the pad rotates with ω_2. Notice that all the points on the wafer are always in contact with the pad, the reverse is not true. We calculate the time that a point on the pad is in contact with the wafer as a function of the distance from the center.

We first consider the case without the oscillatory motion. For each revolution of the pad, the fractional time that a point on the pad spends in contact is the ratio of the lengths between the arc of the circle contained in the wafer and the whole circle. We can also think of this in terms of the angles, as shown in the picture. Since we know h_0, the distance from the center of the pad to that of the wafer, and r, the radius of the wafer, we can compute the angle θ, using the law of cosine. So the fractional time that the point x away from the center of the pad spends inside the wafer in one revolution of the pad is

$$T(x; h_0, r) = \frac{1}{\pi}\cos^{-1}\left(\frac{x^2+h_0^2-r^2}{2xh_0}\right) \quad \textit{whenever} \ |\frac{x^2+h_0^2-r^2}{2xh_0}| \leq 1$$

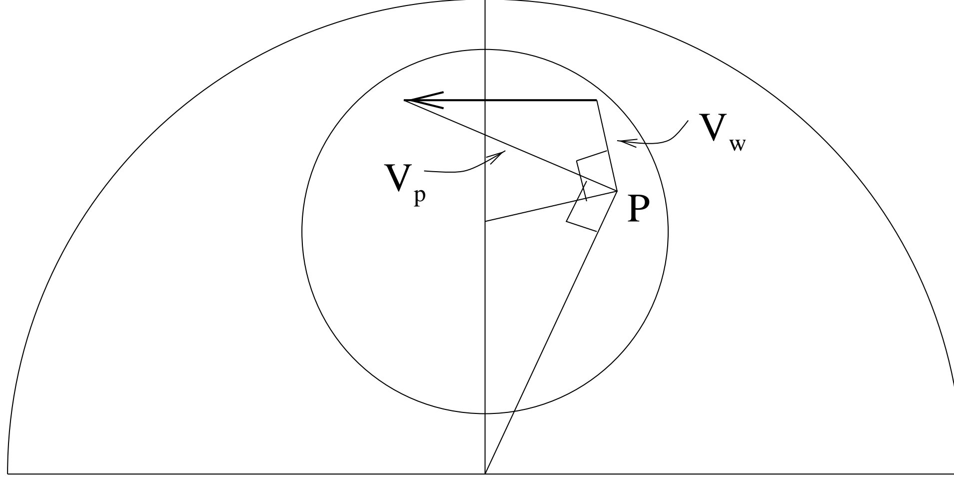

Figure 2: Relative Velocity

This condition holds only for the points on the pad that are in contact with the wafer for some time during a single revolution.

The profile with $r = .2$ and $h_0 = .5$, is shown below in Fig 4.

2.2.2 With oscillatory motion

We assume that the oscillatory motion is slow relative to the spinning of the wafer that the contact time can be approximated by the expression for the stationary case above. This is the case in practice. Typically, $\omega_1 = \omega_2 = 2sec/rev$ and $\omega_h = 15sec/period$.

We introduce another parameter a, half the amplitude of the oscillatory motion. The center of the wafer then moves between $h_0 - a$ and $h_0 + a$. We notice that the errors from the upward and downward movement would cancel each other to some degree. Therefore, we take the average $T(x; h_0, r)$ over one period d of the oscillatory motion.

$$I(x; h_0, r, a) = \frac{1}{d} \int_{t_0}^{t_0+d} T(x; h(s), r)\ ds$$

The position of the center in time can be written as

$$h(t) = h_0 + a\, sin(\omega_h t)$$

We therefore have

$$I(x; h_0, r, a) = \frac{\omega_h}{2\pi} \int_0^{2\pi/\omega_h} \phi(t)\ dt,$$

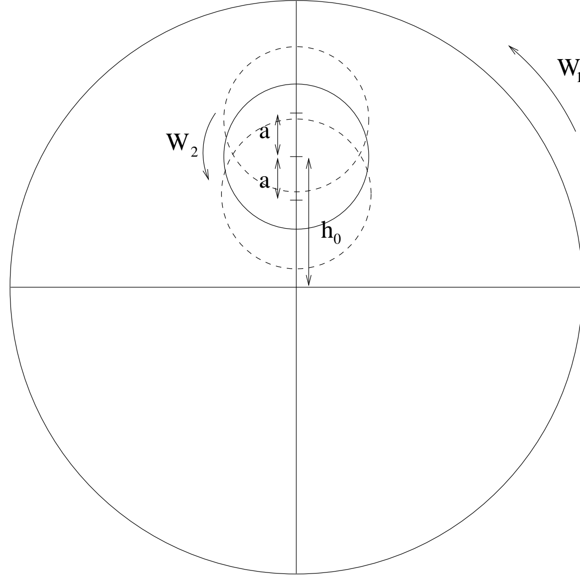

Figure 3: Oscillatory Motion

$$\phi(t) = \begin{cases} 0, & |\psi| > 1 \\ \frac{1}{\pi}\cos^{-1}(\psi), & |\psi| \le 1 \end{cases}$$

$$\text{where } \psi = \frac{x^2 + h(t)^2 - r^2}{2x\,h(t)}$$

We have the two cases as above because for a given point x on the pad, the wafer may move out of range for a part of the period and there is no contribution to the contact time in that case. The profile of contact time with oscillation when h_0=0.5, r=.2 and $\omega_h = 1$ are shown in Fig 5.

2.3 Preston's Law

In our model, we take Preston's law for granted. Preston's law claims that

$$RR_p = C_p\ pV,$$

$$RR_w = C_w\ pV,$$

where RR_p and RR_w are the removal rates for the pad and the wafer respectively, C_p and C_w are the Preston coefficients for the pad and the wafer respectively, p is the pressure, and V the relative speed. This simply says that in the parameter regime in which the CMP takes place, the removal rate varies linearly with the pressure applied and the relative speed. While there is no theoretical

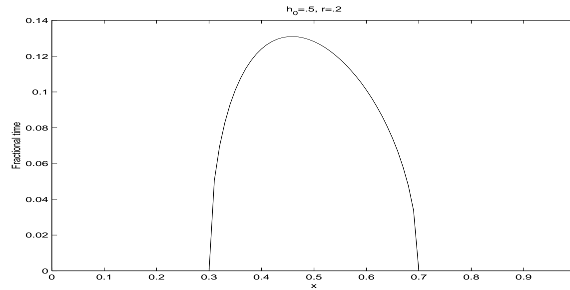

Figure 4: Contact Time (without oscillation)

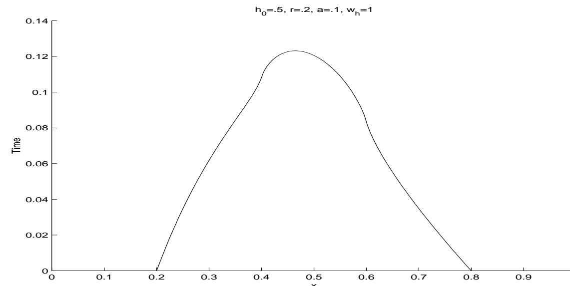

Figure 5: Contact Time (with oscillation)

basis for this assertion, it agrees with our intuition and has been experiementally verified to be a good approximation. These equations are coupled through the common pressure on the contact area between the pad and the wafer.

3 The Model

In the following model we neglect the slurry. Since we are interested in the global planarization, mostly due to the mechanical aspect of the process, this is a reasonable simplification. We also assume that the pad and the wafer are fully in contact. We assume that we start with a flat rigid wafer and a flat elastic pad. Ideally we would like to consider the full three dimensional model. However, due to computational difficulties we reduce the problem to two or one dimensional problem. We first briefly describe the full elasticity model. We would have to solve this set of equations in three dimensions at each time step in order to get the correct behavior.

We fix the bottom of the pad on the xy-plane and the center of the pad at the origin.Also, we assume that the center of the wafer is on the positive x-axis. Let $S_p(x, y; t)$ be the profile of the "elastic" pad, $S_w(\hat{x}, \hat{y}; t)$ the profile

of the "rigid" wafer, S_w determines the distance from the surface of the wafer facing the pad to the bottom of the pad. $P(\hat{x},\hat{y};t)$ the pressure at point $(\hat{x},\hat{y})$, and $V(\hat{x},\hat{y};t)$ the relative velocity, all at time t. The wafer is pushed into the pad by a fixed force F. As a result, the whole wafer is displaced vertically by a constant distance c, and the elastic pad will experience a displacement $u = (u_1(x,y,z), u_2(x,y,z), u_3(x,y,z))$. At this moment, assuming linear elasticity, the pad is in static equilibrium in which we drop any body forces, due to gravity for example. The equilibrium (Navier's) equation in terms of the stress tensor σ (force per unit area) is:

$$\mathrm{div}\sigma = 0 \tag{1}$$

where σ is related to the strain tensor (displacement per unit length) and the displacement vector via the relations:

$$\begin{aligned} \sigma_{ij} &= \lambda\epsilon_{kk}\delta_{ij} + \mu\epsilon_{ij}, \\ \epsilon &= \tfrac{1}{2}(\nabla u + \nabla u^T), \end{aligned}$$

where: $\mu = \frac{E}{2(1+\nu)}$ and $\lambda = \frac{\nu E}{(2(1+\nu)(1-2\nu)}$ are Lame constants, E is the Young's modulus and ν is the Poisson ratio.

Thus the equilibrium (Navier Equation) Eq.(1) can be rewritten in terms of the displacement u as

$$\mu u_{i,jj} + \frac{\mu}{1-2\nu} u_{j,ji} = 0 \tag{2}$$

with boundary conditions:

$$\begin{aligned} u|_{z=0} &= 0, \\ u|_{\{(x,y,S_w(x,y;t)):x^2+y^2\le r^2\}} &= S_p(x,y;t) - S_w(\hat{x},\hat{y};t) + c, \\ \sigma\cdot n|_{\{(x,y,S_p(x,y;t)):x^2+y^2\ge r^2\}} &= 0, \end{aligned}$$

and with the following constraint:

$$\iint_{(x,y,S_w(x,y;t)):x^2+y^2\le r^2} \sigma\cdot n\, dS = \mathbf{F}.$$

where particles (x,y) and $(\hat{x},\hat{y})$ are in contact at time t, and c the vertical movement of the wafer.

Observe that $\mathrm{T} = \sigma\cdot n$ is the traction vector, and n is the outward normal on the surface of the pad.

As noted above, the shape of the pad and wafer are dependent not only on the elastic properties of the materials but the removal rate as well. Expressing $(RR)_p$ to be the removal rate of the pad, $(RR)_w$ to be the removal rate of the wafer, and $T(x,y)$ the "unit-free" contact time of a point (x,y) on the pad with

the wafer.

$$\begin{aligned}\frac{dS_p}{dt} &= -(RR)_p(x,y,t)T(x,y),\\ \frac{dS_w}{dt} &= (RR)_w(\hat{x},\hat{y},t).\end{aligned}$$

By Preston's Law,

$$\begin{aligned}(RR)_p &= \text{removal rate of the pad}\\ &= \frac{\text{(volume of material removed from pad)}}{\text{(unit area)(unit time)}}\\ &= C_pP(x,y,t)V(t),\end{aligned}$$

where $V(t)$ is the relative velocity between the pad and wafer, and C_p is a constant.

Plugging this in to our equations above,

$$\frac{dS_p}{dt} = -C_pP(x,y,t)V(t)T(x,y), \tag{3}$$

$$\frac{dS_w}{dt} = C_wP(\hat{x},\hat{y},t)V(t) \tag{4}$$

With the initial conditions $S_p(x,y,0)=d_0$ and $S_w(\hat{x},\hat{y},0)=d_0$.

Now, since solving this three dimensional system is hard, we reduce it to a two dimensional system. To do so we take a radial section through the pad such taht this ray passes through the center of the wafer see Fig. 6. So Equations (3) and (4) are now:

$$\frac{dS_p}{dt} = -C_pP(x,t)V(t)T(x), \tag{5}$$

$$\frac{dS_w}{dt} = C_wP(\hat{x},t)V(t), \tag{6}$$

$$S_p(x,0)=d_0 \quad , \quad S_w(\hat{x},0)=d_0. \tag{7}$$

3.1 Simplification of the 3D Model

3.1.1 The completely 2D Elastic Model

Now to solve the system we need to find the pressure as a function of the applied force and the resulting displacement. From here we have two alternatives. The first one is to continue with solving the 2D form of Eq. 2 using the Boundary Element Method (BEM).

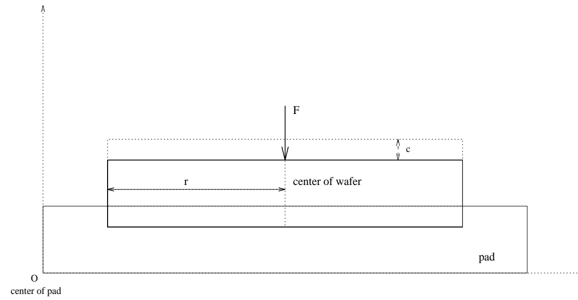

Figure 6: Schematic radial cross section

3.1.2 The Mattress Model

The other alternative is to simplify the system further, by assuming that the pad is a discontinuous elastic body comprised from a set of springs. Each spring is fixed x units away from the center of the pad. In addition each spring has an initial length $S_p(x,t)$. Using Hooke's law, the pressure $P(x,t)$ (force per unit area) can be expressed as

$$P(x,t) = k\left(\frac{c - (S_w(x,t) - S_p(x,t))}{S_p(x,t)}\right) \tag{8}$$

where k denotes Hooke's constant.

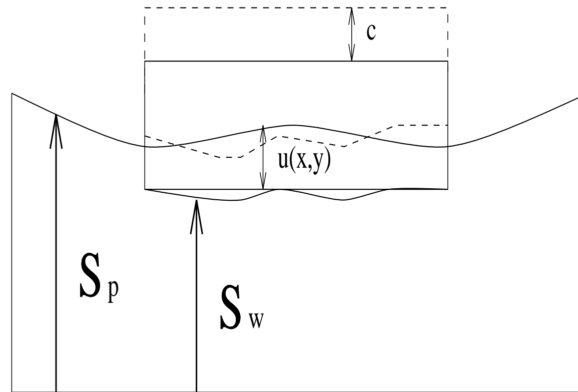

Figure 7: Spring Model

For now, assume homogeneity so the spring constant is independent of time or position. Since the total applied force is $F = \int P(x,t)$, then we can express the constant vertical displacement c when the wafer is pressed into the pad as:

$$c = \frac{(F/k - 2r) + \int S_w/S_p\,dx}{\int 1/S_p\,dx} \tag{9}$$

where r is the radius of the wafer.
Substituting Eqs. (8) and (9) in Equations (5) and (6) we get the so called "mattress model".

4 Numerical Results

4.1 Description of the Method

We first introduce the general formulation of a method for calculating the wear of the pad and the wafer, using Preston's laws. The method needs a subroutine which will compute the pressure distribution underneath the wafer when it is in contact with the pad, given the profiles of the pad and the wafer specified on a grid that will be described in detail below. The method is designed to be compatible with the kinds of spatial discretizations that are often used to compute the pressure distributions from elasticity theory. Note that we are assuming below that the profile of the pad is radially symmetric with respect to the center of the pad, and that the profile of the wafer is radially symmetric with respect to the center of the wafer. We do this for simplicity in both the exposition and in the calculations, but the method can easily be extended to more general profiles.

We discretize the pad in the radial direction, that is we assume we have a set of radial values $\{r_i\}_{i=1}^N$ where the spacing between these values is uniform, $r_{i+1} = r_i + \delta r$. We also assume we have a grid of radial values on the wafer $\{\rho_i\}_{i=1}^M$ where the spacing between the values is also δr. We assume that $\rho_1 = 0$. Corresponding to these different grid points we have the values of the profiles on the grid, that is, two sets of numbers, $\{S_{p,i}\}_{i=1}^N$ and $\{S_{w,j}\}_{j=1}^M$ where $S_{p,i} = S_p(r_i)$ and $S_{w,j} = S_w(\rho_j)$.

From the profiles of the pad and wafer on the specified grid, $S_{p,i}$ and $S_{w,j}$ we can use some numerical procedure to calculate the corresponding pressure distribution between the wafer and the pad when we push the wafer into the pad with some fixed force. The details of how this calculation is performed are not important so long as it is sufficent that the profiles be specified on the grids we have just defined. For the results presented later in this section, we use the spring model described in the previous section. We will take the values of the pressure only at certain distinguished points on the wafer, namely, the points where the different grids intersect, that is points on the wafer $(i,j) = (r = r_i, \rho = \rho_j)$. At each such point the pressure is specified $p(i,j) = p(r_i, \rho_j)$.

In our computations, in order to maintain the radial symmetry of the pad and wafer profiles, we need to ensure that different points on the pad at the same distance r_i from the pad center see the same pressure, and similarly, that points on the wafer at the same distance ρ_j from the wafer center see the same pressure.

But the pressure distribution, as computed above is not radially symmetric on either the pad or the wafer. Thus we will assume that the actual pressure seen by the wafer or pad is the average pressure taken over either an arc of fixed $r = r_i$ across the wafer, or a circle of fixed $\rho = \rho_j$ around the wafer. In particular, $\bar{p}(i)$ is the spatially averaged pressure over the wafer at the distance $r = r_i$ from the wafer center, and $\tilde{p}(j)$ is the spatially averaged pressure around the wafer at a distance $\rho = \rho_j$ from the wafer's center. Replacing the pressure with its average value in Preston's law is justified by the fact that Preston's law is linear in the pressure, and the fact that the time scale of the wearing of the pad should be much longer than one rotation period of pad and wafer, so that it is reasonable to assume that the wearing in one rotation is negligible. Note that the need to average the pressures could be dropped if we were not assuming radial symmetry.

Once we know the effective values of the pressure seen by any point on the pad we can use Preston's laws to compute the wearing of the pad and wafer profiles. The value of the profile at each separate grid point satisfies Preston's law, where the pressure at that grid point is used. The profiles $S_{p,i}$ and $S_{w,j}$ then satisfy the ODEs:

$$\begin{aligned} \frac{dS_{p,i}}{dt} &= -C_p T(d,i)\bar{p}(i)v(d) \\ \frac{dS_{w,j}}{dt} &= C_w \tilde{p}(j)v(d) \end{aligned} \tag{10}$$

Here d is the distance from the center of the pad to the center of the wafer. $T(d,i)$ is the contact time at a distance r_i from the pad center and $v(d)$ is the relative velocity. Note that, if the wafer is oscillating back and forth, then d is a function of time. Note that these form a coupled system of $N + M$ nonautonomous ODEs. They are coupled through the pressure distribution which, at any fixed time, depends on the values of all the heights $S_{p,i}$ and $S_{w,j}$. The basis of our computation for computing the wear of the pad and wafer as time evolves then is to solve (10) numerically.

4.2 Results

We now present some of the results from our computation described above. To compute the pressure distributions, we have used the spring model described in section 3.2. For the pad, we have used a Young's modulus of $E = 4.0 \times 10^7 N/m^2$ and a Poisson ratio of $\nu = 0.4$, and a wearing constant of $C_p = 10^{-13} m^2/N$. Its thickness was 1cm and its radius was 25 cm. The wearing constant of the wafer was $C_w = 7.2985 \times 10^{-14} m^2/N$, which is about the experimentally observed value [3]. The wafer's radius was 10cm. The wafer was pushed into the pad with a total force of 735 N. The period of rotation of pad and wafer was 2s and every wafer was polished for 60 rotations. The wafer oscillated back and forth with a period of 15s and an amplitude of about 1cm.

In figure 8 we show the 20th polished wafer after starting with a flat pad, and in figure 9 we show the 200th wafer polished by the same pad. It is evident

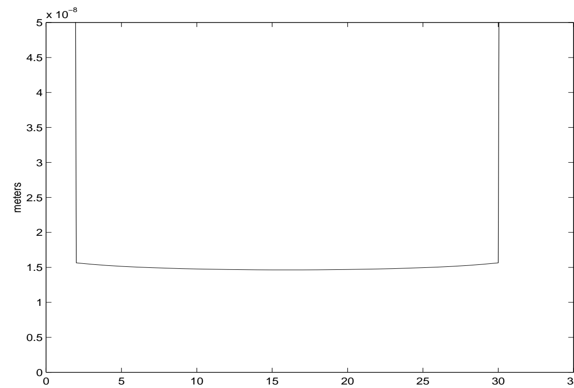

Figure 8: 20th polished wafer

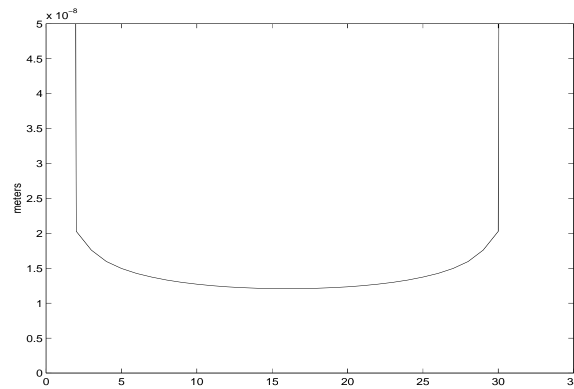

Figure 9: 200th polished wafer

from these pictures that as we continue polishing, the planarity of the polished wafer deteriorates considerably. This is further illustrated by figure 10 which shows how the vertical variation on a wafer increases as the pad keeps polishing. It shows the vertical distance from the highest to lowest point on the wafer for every 20 wafers polished. It is an increasing function, and it is sublinear. The sublinearity indicates that as the pad continues to polish, the deterioration in planarity becomes smaller.

In figure 11 we show the pad after we have polished 200 wafers. The wearing is skewed toward the center of the pad, though not dramatically. This is principally the influence of the contact time, which itself is skewed towards the center of the pad. The basic qualitative shape in figure 11 is confirmed by experimental data, which shows a similar gentle decrease from the edges into the depressed middle, and is also skewed towards the center of the pad. However, there is one

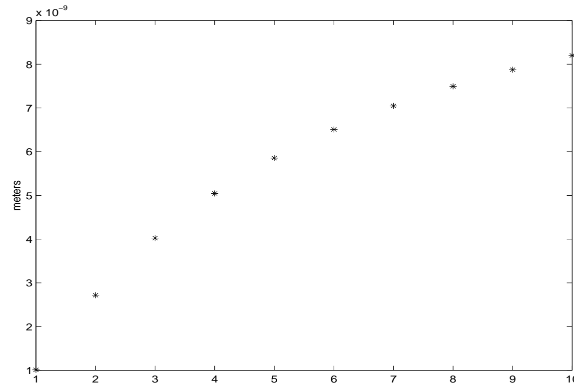

Figure 10: vertical variation in polished wafers

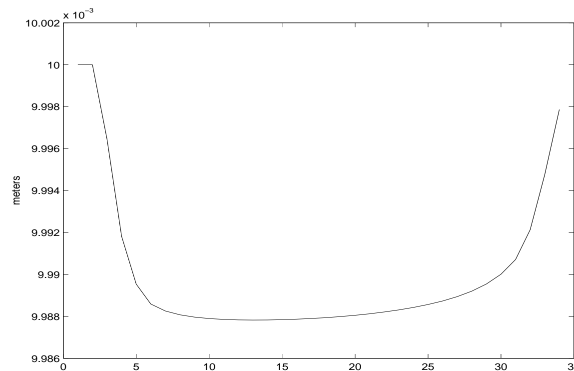

Figure 11: pad after 200 wafers

major quantitative difference: The total wear on the pad here is about a tenth of a percent of the thickness of the pad, whereas in the experimental results it is about 10 or 20 percent.

If we want the pad to wear more we should increase the constant C_p. So, we increased it by a factor of 100 to $10^{-11}m^2/N$ and ran it for 200 wafers. Figure 12 shows the resulting pad profile. Now, we do wear about 10 percent of the total thickness of the pad, but the profile now does not agree with experimental results. The pad profile simply drops at the edges to a flat valley.

Despite the discrepancy with the experimental results, we feel the above results are promising. The case with $C_p = 10^{-13}m^2/N$ agreed qualitatively quite well with empirical results, except that the total amount of wear is far too little. We feel this indicates not a deficiency of the model, but more likely that the actual correspondence between our model and the real physical setup

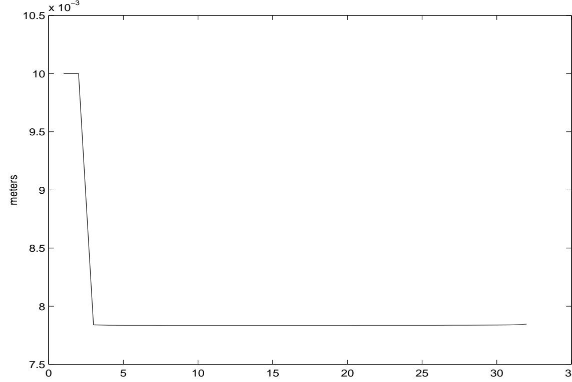

Figure 12: pad after 200 wafers with $C_p = 10^{-11}$

needs to be worked out more carefully. In particular, in the above simulations we have been using a pad that is much too thick. Our pad is 1 cm, but the real pads are about an order of magnitude smaller. More work needs to be done to make the model's parameters agree with realistic physical parameters.

5 Boundary Elements and the Elasticity Model

5.1 Description of the method

The boundary element method (BEM) has been successfully applied in elasticity problems [10, 11, 12].

In order to use the elasticity model, we need to compute the pressure distribution on the surface of the pad due to the applied force at the area of contact with the wafer for a fixed time t.

Since the 3D model is very hard to model numerically, we will compute the pressure distribution only along a common radial cross-section of the pad and the wafer. Hence we consider the 2D model of equation 2 in this section.

The pressure distribution is obtained by computing the stress distribution due to the applied force.

The applied force will be indicated by the resulting displacement on the contact area with the wafer which we will assume to be the whole surface of the wafer facing the pad.

We followed the standard way in [12] [10] in applying the BEM. We briefly describe their technique. The method of weighted residuals is used to approximate the displacement. The fundamental solution is used as the weighting function. The displacement of the fundamental solution is the solution of the Navier's equation (1) due to a source force applied on an interior point $\xi = (x_i, y_i)$ in the direction e_k. In particular these equations are:

$$\mu u_{ki,jj} + \frac{\mu}{1-2\nu} u_{kj,ji} + \delta(x,\xi) e_k = 0$$

The fundamental displacement is the solution of the above equation and has the form:

$$u^*_{ki}(x-x_i, y-y_i) = \frac{1}{8\pi\mu(1-p)} \left(\{(3-4p)\log(1/r) - 0.5\}\delta_{ki} + \frac{\partial r}{\partial x_i}\frac{\partial r}{\partial x_k} \right)$$

The fundamental traction is

$$T^*_{ki}(x-x_i, y-y_i) = -\frac{1}{4\pi(1-p)r} \left[2\frac{\partial r}{\partial n}\frac{\partial r}{\partial x_i}\frac{\partial r}{\partial x_k} + (1-2p)\left(n_k \frac{\partial r}{\partial x_i} - n_i \frac{\partial r}{\partial x_k} + \frac{\partial r}{\partial n}\delta_{ki} \right) \right]$$

The formulation of the weighted residual integrals is

$$\int_\Omega \sigma_{ij,i} u^*_i d\Omega = \int_{\Gamma_1} (T_i - \tilde{T}_i) u^*_i d\Gamma - \int_{\Gamma_2} (u_i - \tilde{u}_i) T^*_i d\Gamma \tag{11}$$

By integrating by parts the term on the left hand side we find :

$$\int_\Omega \sigma_{ij,j} u^*_i d\Omega = \int_\Omega \sigma^*_{ij,j} u_i d\Omega + \int_{\Gamma_1} u_i T^*_i d\Gamma - \int_{\Gamma_2} u_i T^*_i d\Gamma \tag{12}$$

Substituting in the above equation we obtain :

$$\int_\Omega \sigma^*_{ij,j} u_i d\Omega = \int_{\Gamma_1} \tilde{u}_i T^*_i d\Gamma - \int_{\Gamma_1} T_i u^*_i d\Gamma - \int_{\Gamma_2} \tilde{T}_i u^*_i d\Gamma \tag{13}$$

Since the stress tensor due to a body source force in the direction e_k satisfies $\sigma^*_{ij,j} + \delta e_i = 0$ we have ,

$$\int \sigma^*_{ij,j} u_i d\Omega = -e_i u_i(\xi) \tag{14}$$

This will give us the integral equation:

$$u_i(\xi) = \int_\Gamma T_j u^*_{ji} d\Gamma - \int_\Gamma u_j T^*_{ji} d\Gamma \tag{15}$$

The goal is to evaluate the displacement on the boundary. If the point ξ is on the boundary it means that the integral will diverge. Therefore, in evaluating $u(\xi)$ for ξ on the boundary, the boundary is expanded by a half circle of radius ϵ with center at ξ. Then in taking the limit as $\epsilon \to 0$, Eq. 15 will now be:

$$u(\xi) = \lim_{\epsilon\to 0} \left[\int_{\Gamma-\epsilon} T_j\, u^*_{ji} d\Gamma - \int_{\Gamma-\epsilon} u_j\, T^*_{ji} d\Gamma \right] + \lim_{\epsilon\to 0} \left[\int_{S_\epsilon} T_i u^*_{ij} d\Gamma - \int_{S_\epsilon} u_j T^*_{ji} d\Gamma \right] \tag{16}$$

It turns out that

$$\lim_{\epsilon \to 0} \int_{S_\epsilon} T_j u^*_{ji} d\Gamma = 0 \tag{17}$$

and in the case of a smooth boundary we have:

$$\lim_{\epsilon \to 0} \int_{S_\epsilon} u_j T^*_{ij} d\Gamma = -\frac{1}{2} u_j(\xi) \delta_{ij} \tag{18}$$

Hence the boundary integral equation is

$$\frac{1}{2} u_j(\xi) = \int_\Gamma u^*_{ij} T_j d\Gamma - \int_\Gamma T^*_{ij} u_j d\Gamma \tag{19}$$

The boundary is divided into n_e elements. We assumed that the approximated solution is constant on each element with an average value assumed at the midpoint(nodes) of each element. The boundary integral equation is evaluated at node n_j to give:

$$\frac{1}{2} u_j(\xi) = \left[\int_{\Gamma_i} u^*_{ij} d\Gamma_i \right] T_j - \left[\int_{\Gamma_i} T^*_{ij} d\Gamma_i \right] u_j$$

for $i = 1, \cdots, n_e$, giving rise to a linear system of $2n_e \times 2n_e$ equations

$$H_{2n_e \times 2n_e} U_{2n_e \times 1} = G_{2n_e \times 2n_e} T_{2n_e \times 1}$$

where:

$$H_{ij} = 0.5\delta_{ij} + \int_{\Gamma_j} T^*_{ij} d\Gamma \tag{20}$$

$$G_{ij} = \int_{\Gamma_j} u^*_{ij} d\Gamma \tag{21}$$

with boundary conditions of displacement and/or traction being specified at each node. Since the boundary conditions are of mixed type, the system is rearranged to have the form $A_{2n_e \times 2n_e} \mathrm{X}_{2n_e \times 1} = \mathrm{B}_{2n_e \times 1}$ [10, 12]. The unknown values at the boundary are in X and the known values are in B. This system is solved using Gaussian Elimination method[**?**] When the traction and the displacement are known all around, the boundary the stress tensor distribution is computed. The pressure at node n_j is found using the equation $P_j(x) = \frac{1}{3}\mathrm{Trace}(\sigma_\mathrm{j})$ where σ_j is the stress tensor at node n_j.

5.2 Numerical Computations

We applied this method on a radial slice of the pad and the wafer along a common diameter, with the origin being the center of the pad. The pad has radius 0.275m and the diameter of the wafer is 0.2 m with the center of the wafer

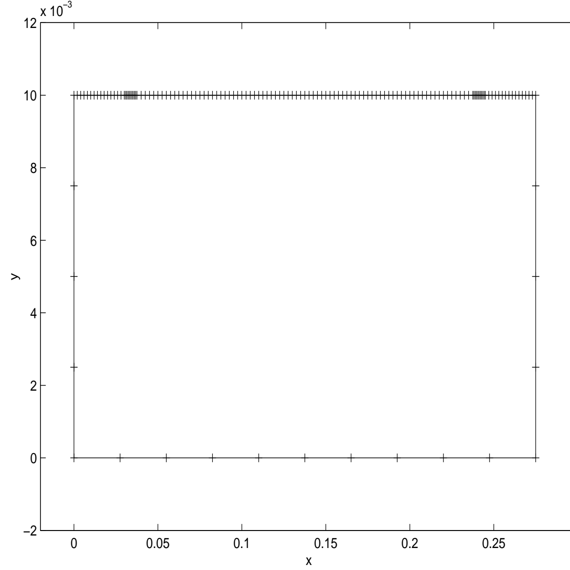

Figure 13: Boundary Element Mesh

0.1375 m from the origin. We specified Young's modulus $E = 4.0 \times 10^7\, N/m^2$ and the pad's Poisson ratio $\nu = 0.4$. We discretized the pad as shown in the Fig. 13. Observe that we set the mesh to be finer on the top of the pad facing the wafer.And it is finest around the region where the top is in contact with edge of the wafer. The boundary condition are specified as follows:

- $u_y = 0, u_x = 0$ if $y = 0$
- $u_x = 0, T_y = 0$ if $0 \leq y \leq 0.01$
- $u_y = 1.5 \times 10^{-9}, u_x = 0$ if $0.0375 \leq x \leq 0.2375$
- $T_x = 0, T_y = 0$ if $0 \leq x \leq 0.0375$ or $0.2375 \leq x \leq 0.275$

The code used in performing the calculations is taken from [10].

5.3 results

1. The vertical displacement on the top of the pad shows that at the edge of the wafer, the pad surface rises as shown in Fig. 14 This is not what one expects that the pad surface should be depressed near the edge of the polishing object and smoothly leveling to the top surface.
2. The pressure (p) is computed using the stress tensor. The pressure curve looks qualitatively correct. As seen in Fig. 15 The pressure is highest

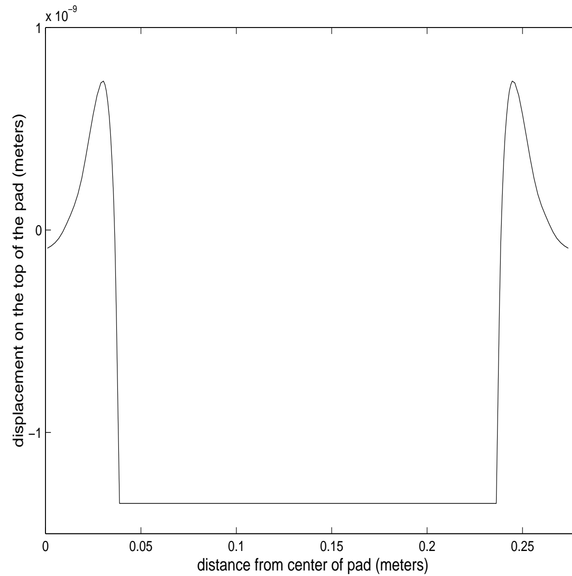

Figure 14: Displacement in Y-direction using BEM

at contact with the edge of the wafer and nearly uniform in the middle.However, the pressure values are negative!

3. The sum of the absolute value of the pressure on the contact area is computed to find the total force corresponding to the imposed vertical displacement. The vertical displacement on the boundary was adjusted until the computed force matches the desired applied force $735\, N/m^2$.

Observe that we applied the above BEM technique only at the first step when the pad and the wafer are both flat. Since the results were not as expected, the method was not implemented to adapt an arbitrary surface of the pad and the wafer. Hence we did not compute the wear out of the pad and the wafer using the 2D elasticity model.

6 Conclusion and Future Work

We have studied the evolution of the wafer and the pad in the CMP process. To our knowledge, this is the first time that a time-dependent computation has been carried out taking into account the oscillation of the wafer and the rotations of both the wafer and the pad. The contact time for the points of the pad was a significant factor in the wear out. The “mattress model” that treats each point as a spring has been used for the solution of the pressure distribution and the wear was determined using Preston’s Law. The results of the numerical

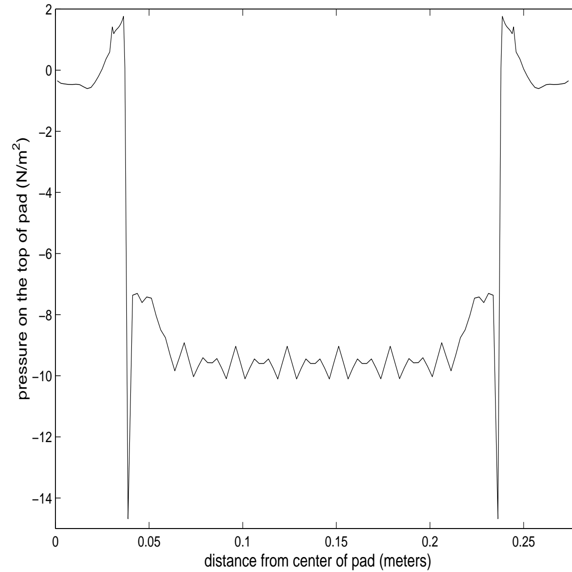

Figure 15: Pressure Distribution using BEM

simulations matched the experimental data provided in a qualitative manner. The surface profiles were comparable and the model predicted the deterioration of the surface qualities for successive wafers. However, it was difficult to draw quantitative conclusions at this point since many parameters, for example the constants used in the Preston's Law, were not known precisely. Calibrating these constants against a portion of the data gave us a good result. As we noted in the introduction, the mechanical aspects of the CMP is crucial for the global planarization and important features of the process have been addressed successfully.

We have tried to improve the determination of the pressure from the wafer and pad profiles by solving the two-dimensional elasticity equations using the Boundary Element Method. The pressure distribution computed from the stress tensor seemed accurate but the displacement predicted by this approach seemed counter-intuitive. This area will be explored for conclusive results in the future and will be incorporated in the dynamics simulation of the whole process. Another area of improvement is consideration of the slurry in this process. Contact mechanics for liquid-solid-liquid interaction has been address in [14], and this and other results can be used to determine the more accurate contact area and pressure distribution.

Acknowledgments

We thank our mentor Len Borucki for introducing this interesting problem to us. We are also grateful to Profs. Santosa and Reitich for organizing this workshop and the Institute for Mathematics and its Applications at the University of Minnesota for financial support.

References

[1] R. DeJule, *Advances in* CMP, Semiconductor International, November (1996), pp. 88–96.

[2] Iqbal Ali, Sudipto R. Roy, and Greg Shinn, *Chemical–Mechanical Polishing of Interlayer Dielectric: A Review*, Solid State Technology, October (1994), pp. 63–70.

[3] J. M. Steigerwald, S. P. Murarka, R. J. Gutmann, *Chemical Mechanical Planarization of Microelectronic Materials*, John Wiley & Sons, New York, NY 1997

[4] G. Nanz, L. E. Camilletti *Modeling of Chemical-Mechanical Polishing: A Review*, IEEE Transactions on Semiconductor Manufacturing, vol. 8, no. 4 (1995) pp.382-389.

[5] J. Tichy, J. Levert, L. Shan, S. Danyluk *Contact Mechanics and Lubrication Hydrodynamics of Chemical-Mechanical Polishing*, submitted to Journal Electrochemical Society.

[6] T. K. Yu, C. C. Yu, M. Orlowski *A Statistical Polishing Pad Model for Chemical-Mechanical Polishing* IEDM (1993), pp. 865–868.

[7] C. Srinvasa–Murthy, D. Wang, S. P. Beaudoin, T. Bibby, K. Holland, and T. S. Cale, *Stress Distribution in Chemical Mechanical Polishing*, Thin Solid Films, 308–309 (1997), pp. 533–537.

[8] Chi–Wen Liu, Bau–Tong Dai, Wei–Tsu Tseng, and Ching–Fa Yeh, *Modeling of the Wear Mechanism During Chemical–Mechanical Polishing*, J. Electrochem. Soc., Vol. 143, No. 2 (1998), pp. 716–721.

[9] O. G. Chekina, L. M. Leer, and H. Liang, *Wear-Contact Problems and Modeling of Chemical Mechanical Polishing*, J. Electrochem. Soc., Vol. 145, No. 6 (1998), pp. 2100–2106.

[10] A. El-Zafrany, *Techniques of the Boundary Element Method*, Ellis Horwood, New York, NY, 1993.

[11] C. A. Brebbia, *The Boundary Element Method for Engineers*, John Wiley & Sons, New York, NY, 1978

[12] S. Takahashi, *Elastic Contact Analysis by Boundary Elements*, Lecture Notes in Engineering, Springer-Verlag, Heidelbert, Germany, 1991

[13] M. E. Gurtin, *An Introduction to Continuum Mechanics*, Mathematics in Science and Engineering, Vol 158, Academic Press, San Diego, CA 1981

[14] Ye. A. Kuznetsov, *Effect of Fluid Lubricant on the Contact Characteristics of Rough Elastic Bodies in Compression*, Wear, 102 (1985), pp. 177–194.